CHAPTER V

RESULTS AND DISCUSION:

$(1-x-y)Bi_{0.5}Na_{0.5}TiO_3–xBi_{0.5}K_{0.5}TiO_3–y\ Bi_{0.5}Li_{0.5}TiO_3$

In this chapter, the results are presented for the investigation of $(1-x-y)Bi_{0.5}Na_{0.5}TiO_3–xBi_{0.5}K_{0.5}TiO_3–yBi_{0.5}Li_{0.5}TiO_3$ (BNKLT) powders and ceramics using combustion technique. There are three parts, (1) effects of calcination temperature and content of x and y on crystal structure and microstructure of BNKLT powders, (2) effects of sintering temperature and amount of x and y on crystal structure and microstructure of BNKLT ceramics, (3) effects of x and y on electrical properties of BNKLT ceramics. The scope of measurement is defined and the results of dielectric, piezoelectric, ferroelectric hysteresis loop (P-E), strain loop (S-E) and conductivity properties are presented and discussed.

Introduction

Piezoelectric ceramics are used in various applications such as actuators and sensors. The most widely used piezoelectric materials are lead-oxide-based, especially $Pb(ZrTi)O_3$. Unfortunately, the toxicity of lead-based materials which contains more than 60% of PZT are concern for environmental considerations [93, 94, 95]. It is necessary to develop lead-free piezoelectric ceramics with excellent piezoelectric properties such as $(Bi_{1/2}Na_{1/2})TiO_3$ (BNT). BNT has attracted much attention due to its large remnant polarization (38 $\mu C/cm^2$) and high Curie temperature (T_c=320 °C). However, when compared to PZT ceramics, BNT ceramics possesses lower piezoelectric properties and present poling difficultly because of their high coercive field (E_c=73 kV/cm) [58,70,96]. For developing higher piezoelectric properties, binary and ternary solid solutions based on BNT were developed and shown to have electromechanical high performance at the MPB. The $1-x(Bi_{1/2}Na_{1/2})TiO_3-x(Bi_{1/2}K_{1/2})TiO_3$ (BNT-BKT) binary system exhobits an MPB between rhombohedral and tetragonal phases at the composition$0.16 \leq x \leq 0.20$, with the highest d_{33} values near~ 157 pC/N for x = 0.20. However, the piezoelectric properties of this solid

solution are not yet comparable to PZT [1]. This ternary system has demonstratedgreat potential and current research is focused on improving the piezoelectric and ferroelectric properties. Yang et al. [15] found that doping with BLT could reduce the coercive field and improve the piezoelectric properties of BNT-BKT ceramics, which were as follows: P_r=31.92μC/cm^2, E_c=32.4 kV/cm, d_{33}=203 pC/N and k_p=31.0% with composition of $0.68Bi_{0.5}Na_{0.5}TiO_3$-$0.22Bi_{0.5}K_{0.5}TiO_3$-$0.10Bi_{0.5}Li_{0.5}TiO_3$ ceramic.

The composition $(1\text{-}x\text{-}y)Bi_{0.5}Na_{0.5}TiO_3$–$xBi_{0.5}K_{0.5}TiO_3$–$yBi_{0.5}Li_{0.5}TiO_3$ (BNKLT) can be synthesized using conventional solid state methods with the calcination and sintering temperature of 850-900 °C for 2-4 h and 1100-1200 °C for 2-3 h [8, 9]. It is commonly understood that the conventional solid state method requires compulsory grinding of different oxide mixtures for long periods of time as well as sintering. In addition, the synthesized component distributions are not homogeneous and particle sizes are relatively large. Recently, our previous works have successfully fabricated high quality different oxide ceramics which featured a novel method for materials synthesis for compounds such as $(Ba_{1-x}Sr_x)(Zr_xTi_{1-x})O_3$ [20], $0.79Bi_{0.5}Na_{0.5}TiO_3$-$0.18Bi_{0.5}K_{0.5}TiO_3$-$0.03BiFeO_3$ [97] $(Pb_{1-x}Ba_xTiO_3)$ [22]. This method offers several distinct advantages, with a homogeneous mixture of several components at atomic level, a simple preparation process, low firing temperature and a short dwell time [24, 25, 26]. However, from a survey of the literature, BNKLT ceramics prepared by the combustion method and understanding its strain nature have not been studied. Thus, in this work, $(1\text{-}x\text{-}y)Bi_{0.5}Na_{0.5}TiO_3$–$xBi_{0.5}K_{0.5}TiO_3$–$yBi_{0.5}Li_{0.5}TiO_3$($0.18\leq x\leq 0.26$ and $0\leq y\leq 0.12$) powders and ceramics were prepared by the combustion method, and their microstructure, phase transformation and electrical properties (dielectric, piezoelectric, P-E and S-E loops) were studied systematically.

Experimental

$(1\text{-}x\text{-}y)Bi_{0.5}Na_{0.5}TiO_3$-$xBi_{0.5}K_{0.5}TiO_3$-$yBi_{0.5}Li_{0.5}O_3$ ceramics ($0.18\leq x\leq 0.26$, fixed x=0.10 and $0\leq y\leq 0.12$, fixed y=0.20) (abbreviated as BNKLT x/0.10 and BNKLT y/0.20) were prepared by the combustion technique.Bi_2O_3, Na_2CO_3, K_2CO_3, TiO_2 and Li_2O_3were used as starting materials. According to the formula of BNKLT (11),

stoichiometric amount of raw materials were mixed together with fuel (glycine) in an agate mortarby use of a 2:1 ratio.The mixed powders were calcined between 600 and 850 °C for 2 h.The crystal structure of the calcined powders was detected by X-ray diffraction. The calcined powders were mixed with polyvinyl alcohol and pressed into discs with a diameter of 15 mm under 150 MPa. These pellets were subsequently sintered between900 °C and 1050 °C for a 2 h dwell time with a heating/cooling rate of 5 °C/min.

$$(1\text{-}x\text{-}y)/4Na_2CO_3+x/4K_2CO_3+y/4Li_2CO_3+0.25Bi_2O_3+TiO_2\rightarrow$$
$$(1\text{-}x\text{-}y)Bi_{0.5}Na_{0.5}TiO_3\text{-}xBi_{0.5}K_{0.5}TiO_3\text{-}yBi_{0.5}Li_{0.5}TiO_3+0.25CO_2 \quad (11)$$

The crystal structure of both the calcined powders and sinteredsamples were characterized byX-ray diffraction (XRD). The fracture surface of each sample wasobserved using scanning electron microscopy (SEM). The grain size of each sample was measured by a mean linear intercept method from the SEM micrographs. For electrical measurements, two parallel surfaces of sintered ceramics were polished. Silver paste (Heraeus C1000) was fired on both sides in air at 650 °C for 30 minutes. Dielectric constant and loss of the ceramics for a wide variety of frequencies was measured using LCR meter (Agilent 4284A). Polarization and strain hysteresis measurements were made using a Sawyer-Tower circuit-based system (Radiant Technology Premier II utilizing Vision software).

Result and Discussion

Effect of calcination temperature and content of x and y on crystal structure and microstructure of BNKLT powders

The XRD pattern of BNKLT-0.18/0.10 and BNKFT-0.20/0.05 powders with various calcination temperature between 600 °C and 850 °C for 2 h. The diffraction patterns were indexed on the basis of a rhombohedral structure matched with JCPDS file number 360340. Impurity phases of $K_4Ti_3O_8$and $K_2Ti_6O_3$were discovered at calcinationtemperatures below 750 °C (Figure 43). The pure rhombohedral perovskite phase was found at a calcined temperature of 750 °C, as shown in

Figure 43. The results of BNKLT-0.20/0.10, BNKLT-0.22/0.10, BNKLT-0.24/0.10, BNKLT-0.26/0.10, BNKLT-0.20/0, BNKLT-0.20/0.03, BNKLT-0.20/0.07, BNKLT-0.20/0.10 and BNKLT-0.20/0.12 were similar to BNKLT-0.18/0.10 and BNKLT-0.20/0.05.The percentage of perovskite phase can be calculated by using the equation (12) and the major XRD peak intensities of the perovskite. Here I_{perov}, $I_{K_4Ti_3O_8}$ and $I_{K_2Ti_6O_3}$ refer to the intensity of the (110) perovskite and the intensity of impurity phase of $K_4Ti_3O_8$ and $K_2Ti_6O_3$ peaks, respectively. The increase of phase purity with increasing calcination temperatures is evident. The highest percentage was observed in powders calcinedabove 750 °C,are shown in Table 10-13.The lattice parameter was calculated first by indexing the diffractogram according to hexagonal unit cell and the resulting parameters were then converted to the rhombohedral. The lattice parameter a of all the samples increased with an increase of calcinations temperature. It is because of the powders exist in a more strained form within the atomic entities in non-equilibrium positionsat low calcining temperatures, which relax to the equilibrium positions at higher temperatures.

$$\%\,Perovskite\ phase = \left(\frac{I_{Perov}}{I_{Perov} + I_{K_4Ti_3O_8} + I_{K_2Ti_6O_3}} \right) \times 100 \qquad (12)$$

Figure 44 shows SEM images of BNKLT-0.18/0.10 and BNKLT-0.20/0.05 calcined between600 °C and 850 °C. All the particles consisted of an agglomerated spherical shape. The average particle size increased from 357 nm to 397 nm for BNKLT-0.18/0.10 and 367 nm to 431 nm for BNKLT-0.20/0.05 with an increase in calcination temperature from 600°C to 850°C, are listed in Table 10-13.

The calcination temperature of 750 °C for 2 h. was chose in all compositions and it was then that the amounts of x and y on the crystal structure and microstructure were examined. The XRD diffraction patterns of BNKLT-x/0.10 and BNKLT-0.20/y powders in the range of 10°–60°are shown in Figure 45(a) and 45(b), respectively. The crystal structures of the BNKLT-x/0.10 and BNKLT-0.20/y powders were proposed as a rhombohedral phase, which could be matched with the JCPDS file number 36-0340. When increase of x and y content, the position corresponding to

the characteristic (110) peak shifts towards a lower angle, as shown in Figure 45(a) and 3(b). The lattice parameter of aincreased with increasing x and y content, are listed in Table 10-13.

The morphological changes in the BNKLT-x/0.10 and BNKLT-0.20/y powders formed by combustion technique are exhibited. In general, the particles are spherical in shape and agglomerated. With an increase of x content from 0.18 to 0.26, the average particle size decreases from 367 nm to 232 nm (Table 10 and Table 11). As the y content increased from 0 to 0.12, the average particle size increased from 270 nm to 347 nm (Table 12 and Table 13).

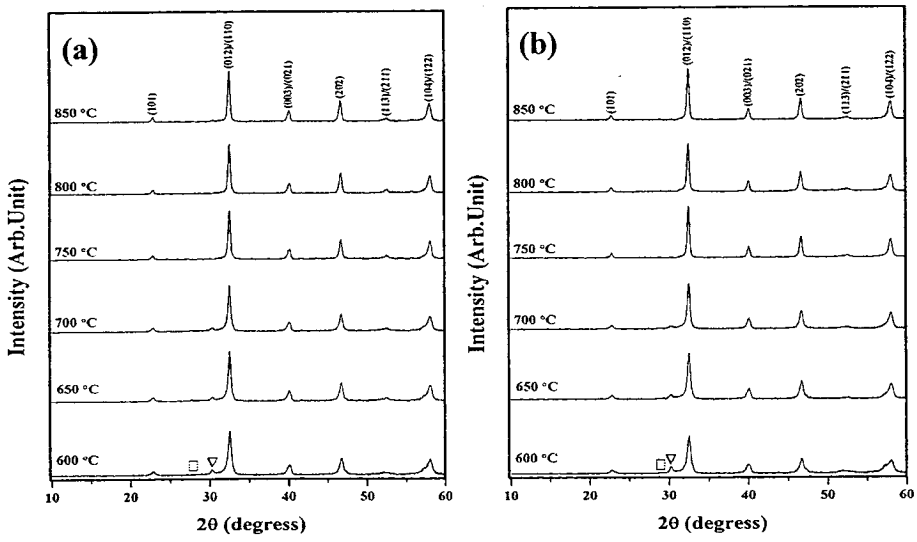

Figure 43 XRD patterns of (a) BNKLT-0.18/0.10 and (b) BNKLT-0.20/0.05 powders calcined at various temperatures for 2 h: (∇ $K_4Ti_3O_8$) and (□ $K_2Ti_6O_3$)

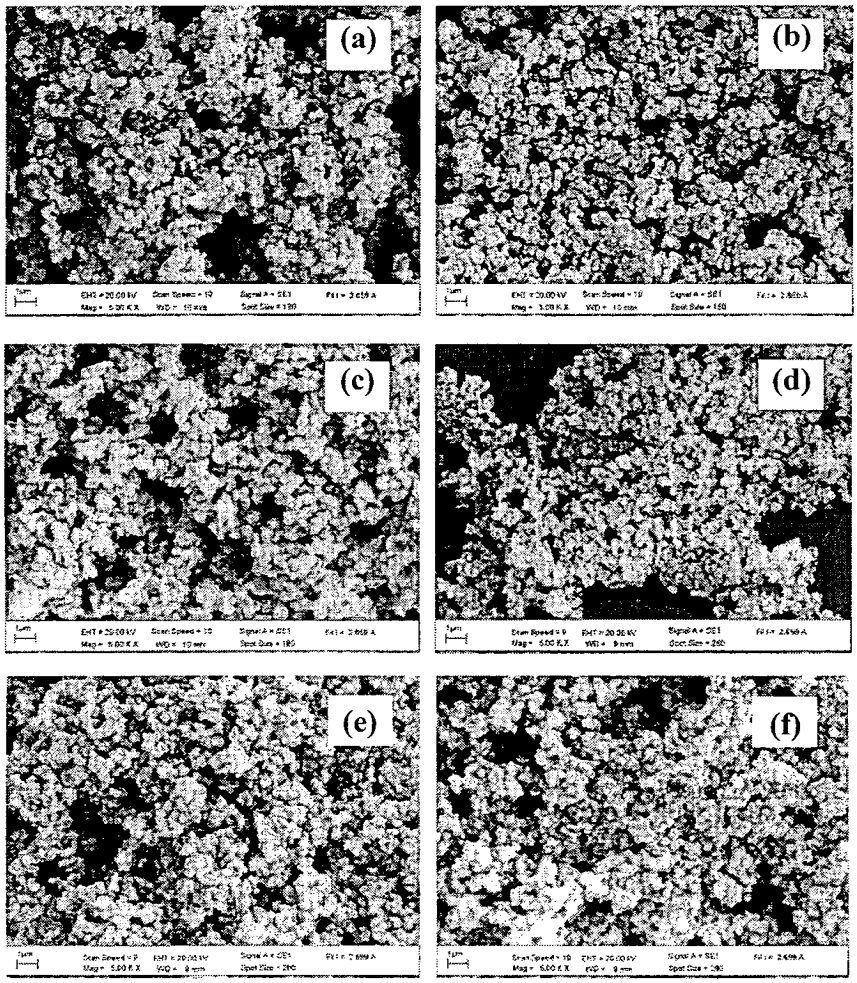

Figure 44 SEM images of BNKLT-0.18/0.10 calcined at (a) 600 °C, (b) 700 °C, (c) 800 °C and BNKLT-0.20/0.05 calcined at (d) 600 °C, (e) 700 °C, (f) 800 °C

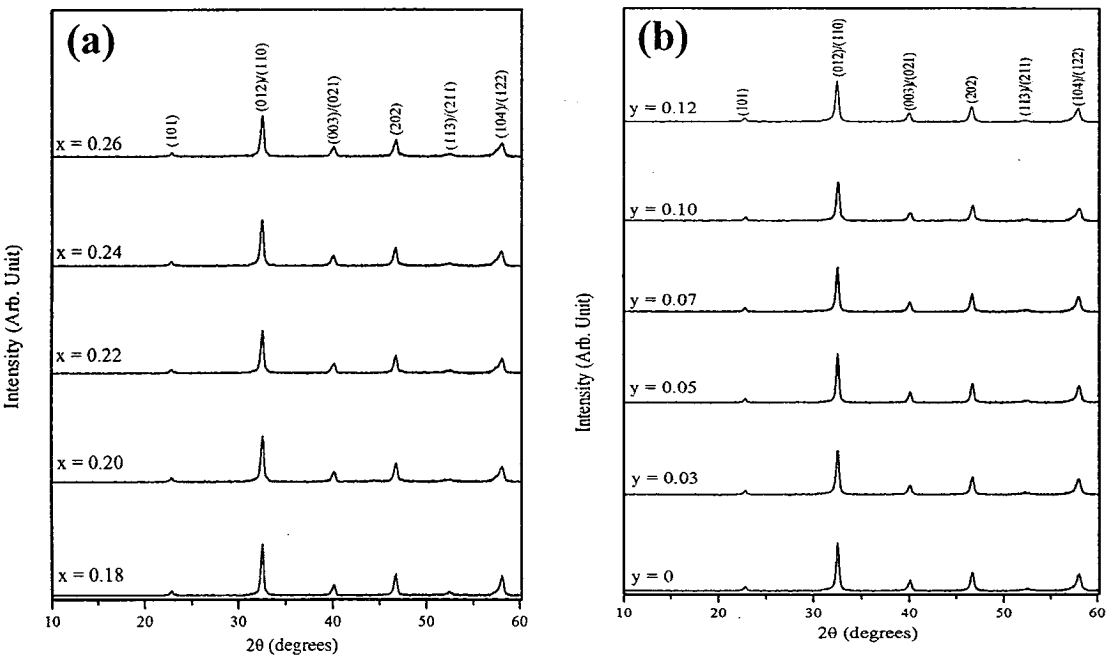

Figure 45 X-ray diffraction patterns of (a) BNKLT-x/0.10 and (b) BNKLT-0.20/y calcined powders

Table 10 Perovskite phase, lattice parameter and average particle size of BNKLT-x/0.10 powders calcined at various temperatures

Composition of x	Calcination temperature (°C)	Perovskite phase (%)	Lattice parameter a (Å)	Average particle size (nm)
0.18	600	84.0	3.8491±0.034	357±14.5
	650	86.0	3.8495±0.066	364±18.1
	700	87.0	3.8595±0.065	367±19.3
	750	100	3.8595±0.035	385±15.4
	800	100	3.8597±0.023	393±13.7
	850	100	3.8591±0.035	397±17.1
0.20	600	79.0	3.8491±0.035	368±18.5
	650	85.0	3.8497±0.021	372±17.5
	700	88.0	3.8498±0.065	383±17.2
	750	100	3.8596±0.045	391±12.8

Table 10 (cont.)

Composition of x	Calcination temperature (°C)	Perovskite phase (%)	Lattice parameter a (Å)	Average particle size (nm)
	800	100	3.8618±0.035	417±18.2
	850	100	3.8624±0.066	423±18.5
0.22	600	83.0	3.8452±0.034	346±13.4
	650	81.0	3.8589±0.045	339±16.1
	700	90.0	3.8490±0.056	371±10.2
	750	100	3.8658±0.074	400±19.2
	800	100	3.8628±0.055	419±17.3
	850	100	3.8628±0.036	420±10.4

Table 11 Perovskite phase, lattice parameter and average particle size of BNKLT-x/0.10 powders calcined at various temperatures

Composition of x	Calcination temperature (°C)	Perovskite phase (%)	Lattice parameter a (Å)	Average particle size (nm)
0.24	600	80.0	3.8575±0.055	319±12.5
	650	83.0	3.8579±0.045	327±10.2
	700	87.0	3.8581±0.056	349±18.6
	750	100	3.8662±0.035	375±13.8
	800	100	3.8689±0.045	389±17.5
	850	100	3.8762±0.056	429±19.6
0.26	600	80.1	3.8645±0.046	310±10.5
	650	82.9	3.8675±0.045	333±19.6
	700	87.7	3.8724±0.055	360±11.5
	750	100	3.8775±0.066	361±18.6
	800	100	3.8798±0.056	373±13.7
	850	100	3.8893±0.045	411±12.5

Table 12 Perovskite phase, lattice parameter and average particle size of BNKLT-0.20/y powders calcined at various temperatures

Composition of y	Calcination temperature (°C)	Perovskite phase (%)	Lattice parameter a (Å)	Average particle size (nm)
0	600	86.0	3.8486±0.035	367±14.4
	650	86.1	3.8495±0.066	354±10.3
	700	87.0	3.8454±0.094	357±10.2
	750	100	3.9595±0.26	363±15.1
	800	100	3.9597±0.033	393±13.0
0.03	600	74.0	3.8491±0.066	357±14.1
	650	86.2	3.8491±0.033	368±16.2
	700	93.0	3.8497±0.045	372±15.4
	750	100	3.9498±0.036	374±11.1
	800	100	3.8596±0.033	381±10.2
0.05	600	76.3	3.8518±0.033	367±13.0
	650	81.1	3.8524±0.066	372±19.1
	700	83.0	3.8542±0.066	386±13.4
	750	100	3.8589±0.052	387±13.3
	800	100	3.8590±0.038	431±10.2

Table 13 Perovskite phase, lattice parameter and average particle size of BNKLT-0.20/y powders calcined at various temperatures

Composition of y	Calcination temperature (°C)	Perovskite phase (%)	Lattice parameter a (Å)	Average particle size (nm)
0.07	600	77.3	3.8658±0.045	370±19.2
	650	82.9	3.8675±0.033	389±10.4

Table 13 (cont.)

Composition of y	Calcination temperature (°C)	Perovskite phase (%)	Lattice parameter a (Å)	Average particle size (nm)
	700	87.7	3.8674±0.033	380±13.3
	750	100	3.8678±0.033	389±12.1
	800	100	3.8679±0.072	427±10.3
0.10	600	79.0	3.8491±0.34	368±18.4
	650	85.0	3.8497±0.066	372±17.4
	700	88.0	3.8498±0.066	383±17.1
	750	100	3.8596±0.035	391±12.2
	800	100	3.8618±0.032	417±18.2
0.12	600	82.9	3.8655±0.033	361±17.3
	650	87.7	3.8724±0.066	360±11.4
	700	89.1	3.8775±0.066	363±18.3
	750	100	3.8798±0.033	453±10.4
	800	100	3.8883±0.034	461±13.4

Effect of sintering temperature and amount of x and y on crystal structure and microstructure of BNKLT ceramics

The XRD diffraction pattern of BNKLT-0.22/0.10 sintered ceramics at various temperatures (900 °C to 1050 °C) are shown in Figure 46.It was found that the BNKLT-0.22/0.10 ceramics possess a single-phase perovskite structure in all samples. All the peaks of the solid solution system were indexed by pattern matching based on JCPDS data on BNT (36-0340)and $Bi_{0.5}K_{0.5}TiO_3$ (36-0339). At sintering temperature of 900 °C, splitting of a (003)/(021) peaks was detected in the 2θ range of 39-41° (Figure 46(b)) and the (202) peak was asymmetric in the range of 45-48° (Figure 46(c)). When sintering temperature is increased, the (003)/(021) peak begins to merge into a single (111) peak and the (202) peak starts to split into two peaks of (002)/(200). This indicated the coexistence of rhombohedral and tetragonal phases, which is consistent with the nature of the specimen with an MPB composition.

Figure 47 demonstrates SEM photographs of BNKLT-0.22/0.10 surfaces and fractures sintered ceramics at various temperatures.. In general, the ceramics showed a quasi-cubic morphology with clear grain boundaries. The morphology of the ceramics is similar to result of BNKLT prepared by solid state reaction method [16]. Increasing the sintering temperatures helped the grains grow. The average grain size increased from 0.87 to 1.39 μm (Table 14). At 950 °C, a porous microstructure with small grain size is observed (Figure 47(b)). The increase in sintering temperature significantly promoted the grain growth and microstructure densification. However, at sintering temperature above 1025 °C, sharpness was reduced (Figure 47(d)).

The density and shrinkage of BNKLT-0.22/0.10 ceramics with sintering temperatures between 900 °C and 1050 °C can also be seen in Table 14.The density and shrinkage increased with increasing sintering temperatures from 1050–1150°C, reached a maximum value at 1025°C and decreased after further sintering at a higher temperature (1050°C). The decrease in density at a high temperature (1050°C) may be due to the bismuth oxide evaporation, and the presence of a porous microstructure.

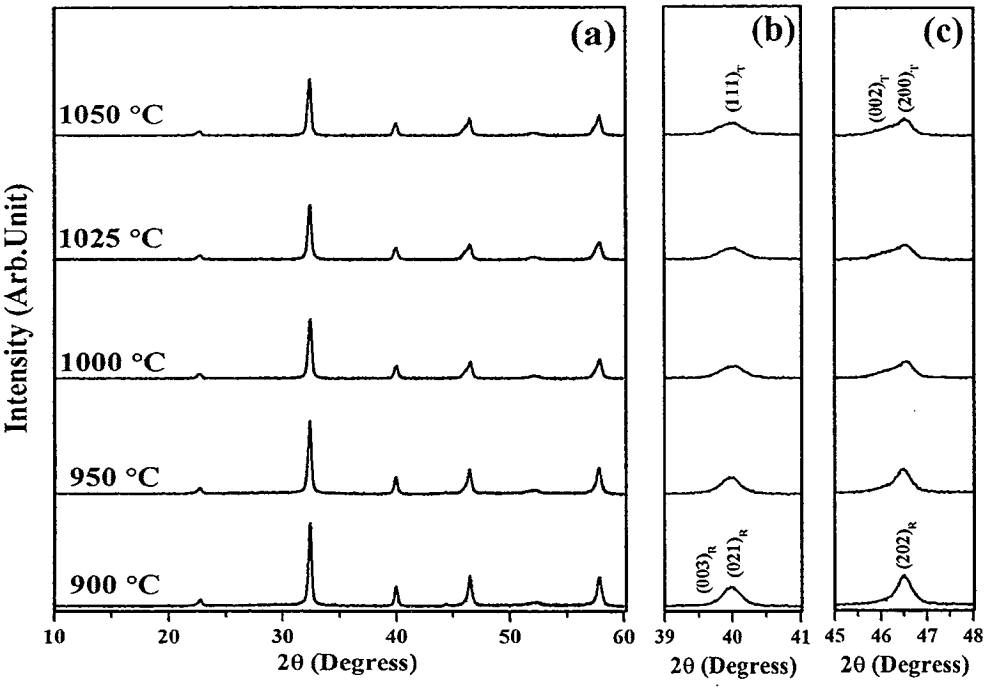

Figure 46 X-ray diffraction patterns of BNKLT-0.22/0.10 sintered ceramics in the 2θ rang of (a) 10° to 60°, (b) 39° to 41° and (c) 45° to 48°

The dielectric constant of BNKLT sintered ceramics as a function of temperature at a frequency of 1 kHz is shown in Figure 48. The dielectric constant showed two peaks (T_d at low temperature and T_c at high temperature) in all samples. T_d is the temperature at which the transition from ferroelectric (rhombohedral) to anti-ferroelectric (tetragonal) occurred. T_c is the temperature at which the phase transition from anti-ferroelectric (tetragonal) to paraelectric (cubic) occurred. When sintering temperature increased from 900°C to 1050°C, the T_d of the samples shifted to the higher temperature from 90°C to 122°C whereas the T_c shifted to lower temperature regions from 339°C to 313°C (Figure 48 and listed in Table 14). The maximum dielectric at T_c increased from 2,364 to 4,344 (highest at 1025 °C) and then drop to 3,968. The maximum results of dielectric constant and density corresponded, which was found at 1025 °C.

The optimum sintering temperature of all samples was chosen at 1025°C for 2 h, and it was then that the amounts of x and y on the crystal structure and microstructure were examined. The XRD patterns of BNKLT-x/0.10 ceramics are shown in Figure 49(a-c). It can be seen that BNKLT ceramics possess a single-phase perovskite structure overall of the compositions in this study which indicates that K^+, Bi^+ and Li^+ ions diffuse into BNKT lattices to form solid solutions. As the x (BKT) content increased, the (110) peak in the BNKLT ceramics gradually shifted to the lower 2θ angles because the K^+ion (1.64 Å) has a larger radius than Na^+(1.39 Å).Generally, the rhombohedral structure is characterized by double peaks of (003)/(021) spitting between 39° and 41° and a single peak of (202) between 45° and 48° whereas a pure tetragonal structure is characterized by a single peak of (111) between 39° and 41° and (002)/(200) peaks splitting between 45° to 48°. At x=0.18, splitting of XRD peaks over the 2θ range of 39°-41° andan asymmetry inthe (202) peak over the range of 45° to 48° was detected. When there was an increase inx content, the peaks merged into one and the (202) peak exhibited a weak splitting into two peaks (002)/(200). This suggests the coexistence of rhombohedral and tetragonal phases, which is consistent with the nature of the specimen with an MPB composition. In the case of y (BLT) additional content, the structure showed the same trend with x addition, as shown in Figure 49. The resultant structure was different than the previous

works, where the addition of y content in all compositions had no effect on the crystal structure [15, 95].

The SEM micrographs of BNKLT-x/y ceramics are shown in Figure 51(a-c). All ceramics show a quasi-cubic morphology and porous microstructure distribution. After polished and thermally etched surfaces, all the specimens become more spherical and dense microstructure, as shown in Figure 52. The average grain size decreased from 1.34 μm to 0.81 μm when the x content was increased from 0.18 to 0.26, as listed in Table 15. It is because of the K^+ concentrates near grain boundaries resulting in decreasing of their mobility. The reduction in the mobility of the grain boundary weakens the mass transport. On the other hand, the grain size increases as the content of y. As is generally recognized, the emergence of oxygen vacancies is favorable to the mass transport during sintering, and greatly promotes the grain growth. The emergence of oxygen vacancies is strongly dependent upon the site occupation of the doping cations in the ABO_3-perovskite structure [95]. Thus, we believe that the element Li^+ enters into the six fold coordinated B-site of perovskite structure to substitute for Ti^{4+}.

Table 14 Average grain size,ρ,ε_r, tanδ, T_d, $T_c$and shrinkage of BNKLT-0.22/0.10 ceramics at various temperatures

Sintering temperature (°C)	Average grain size (μ)	ρ (g/cm^{-3})	ε_r	tanδ at T_c	T_d (°C)	T_c (°C)	Shrinkage (%)
900	0.87	4.99	2,364	0.05	90	339	11.1
950	0.91	5.31	3,611	0.09	114	320	12.7
1000	1.12	5.55	3,634	0.04	111	311	17.3
1025	1.33	5.79	4,344	0.05	107	304	18.4
1050	1.39	5.61	3,968	0.04	122	313	17.9

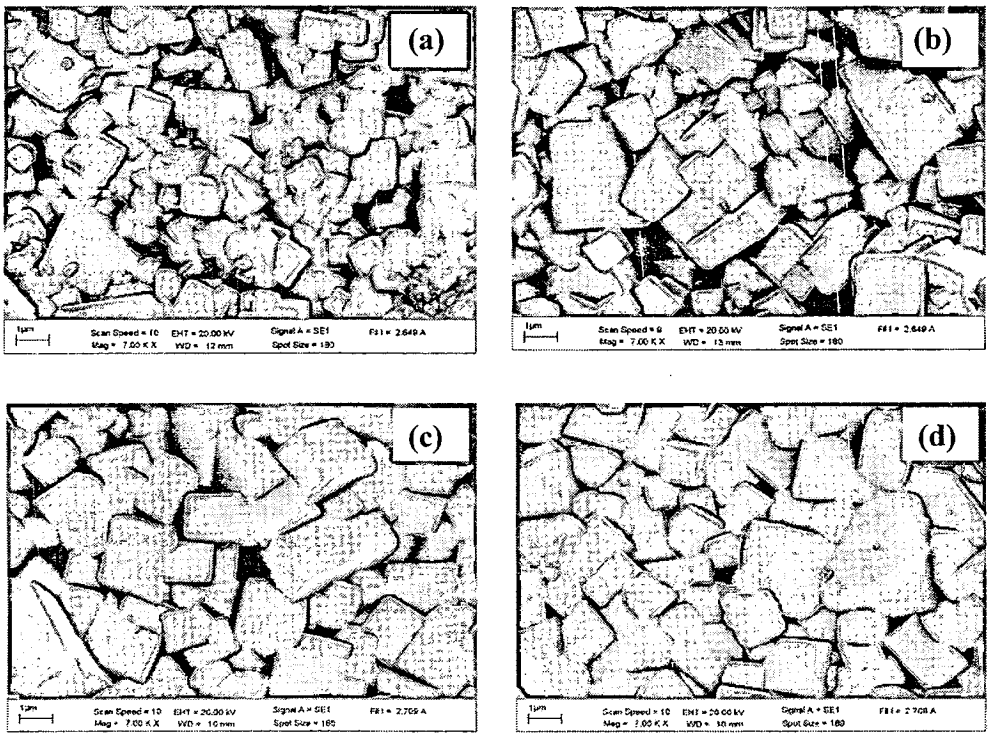

Figure 47 Surface morphologies micrographs of the BNKLT-0.22/0.10 sintered ceramics at various temperatures:
(a) sintered at 950 °C, (b) sintered at 1000 °C,
(c) sintered at 1025 °C, and (d) sintered at 1050 °C

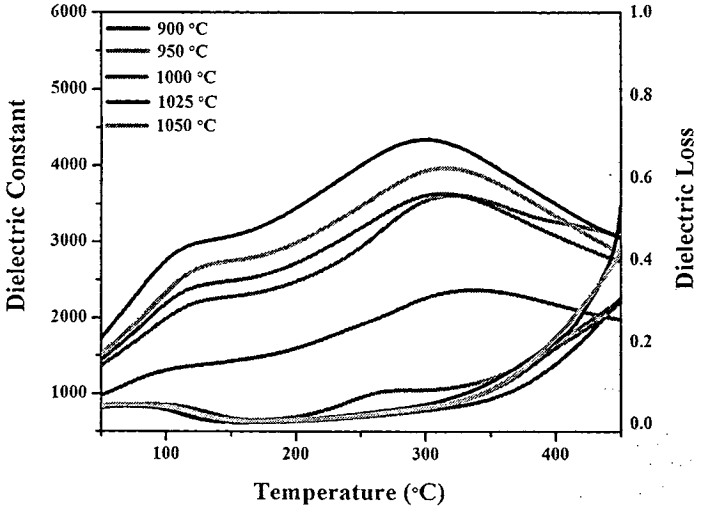

Figure 48 The temperature dependences of dielectric constant (ε_r) of the BNKLT-0.22/0.10 and ceramics at differences temperature

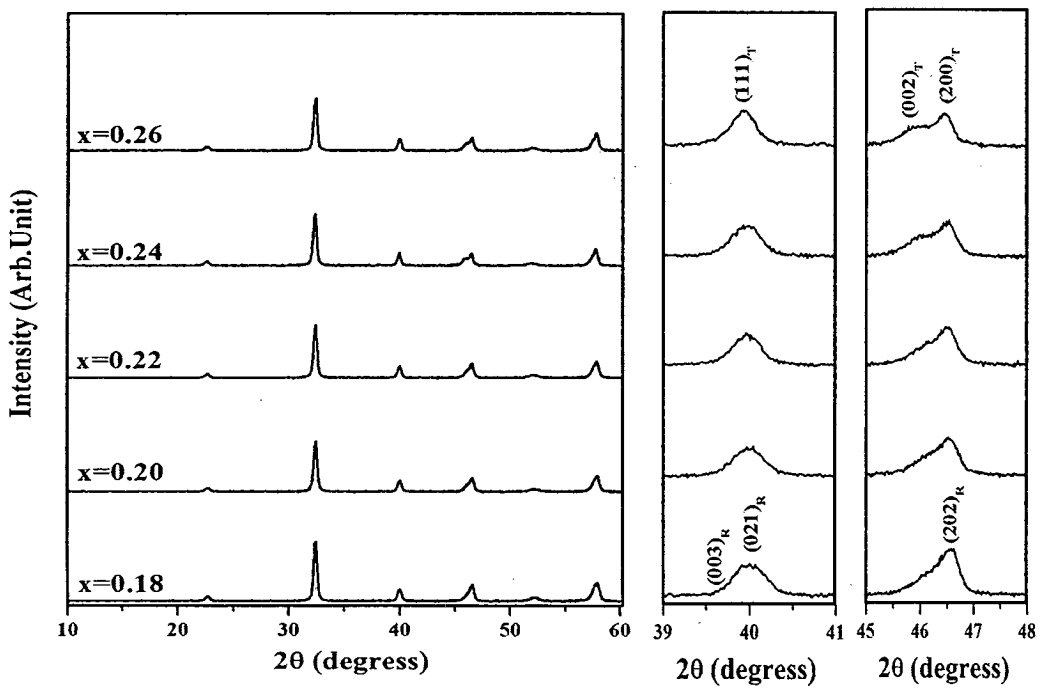

Figure 49 X-ray diffraction patterns of BNKLT-x/0.10 sintered ceramics at different x content

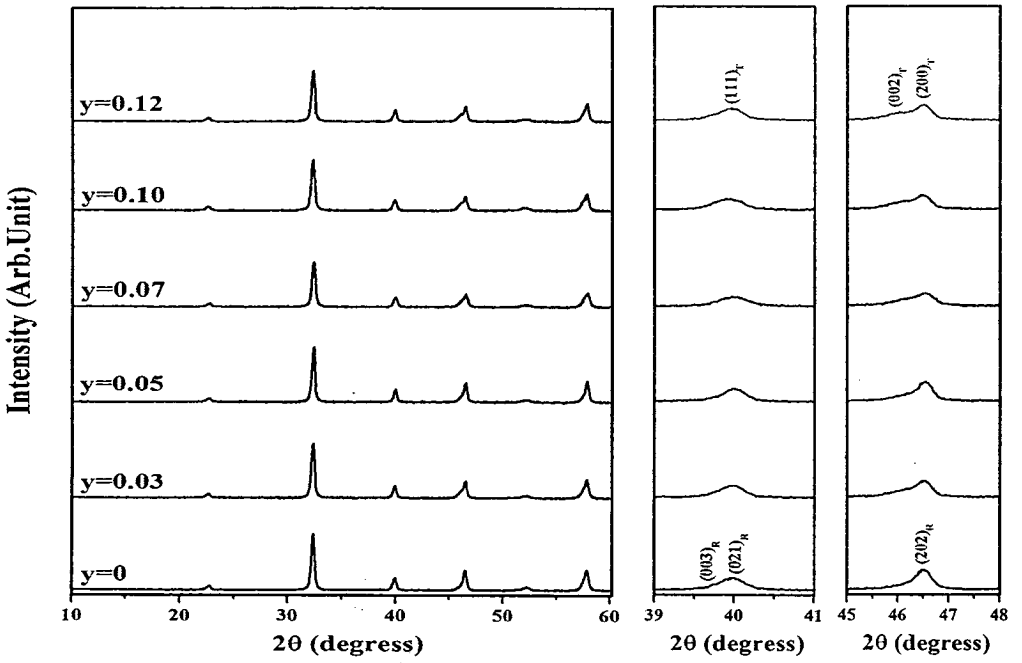

Figure 50 X-ray diffraction patterns of BNKLT-0.20/y sintered ceramics at different y content

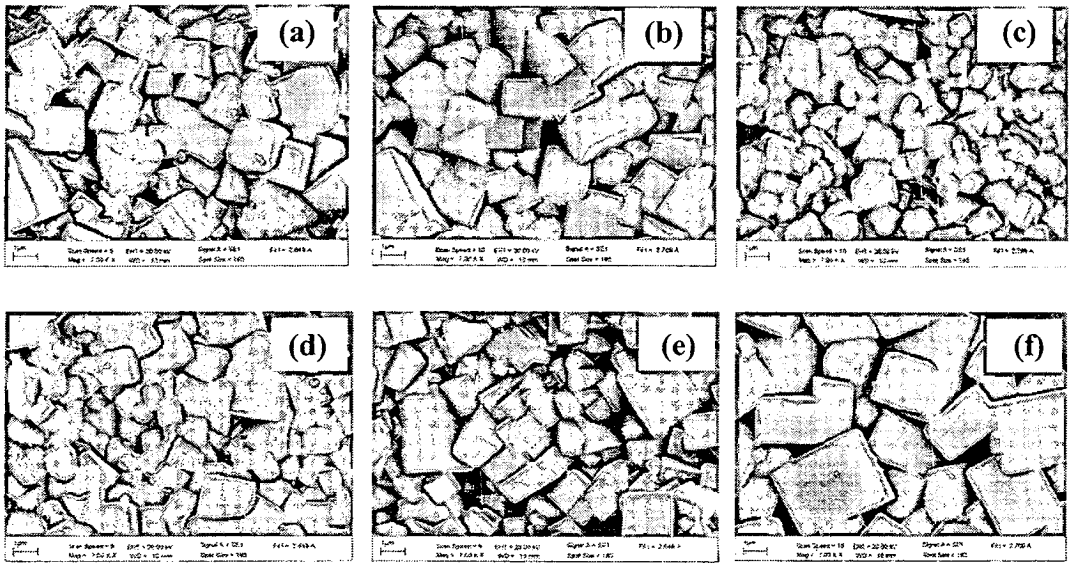

Figure 51 SEM images of BNKLT-x/y sintered ceramics with (a) x= 0.18, (b) x=0.22, (c) x=0.26, (d) y=0, (e) y=0.07 and (f) y=0.12

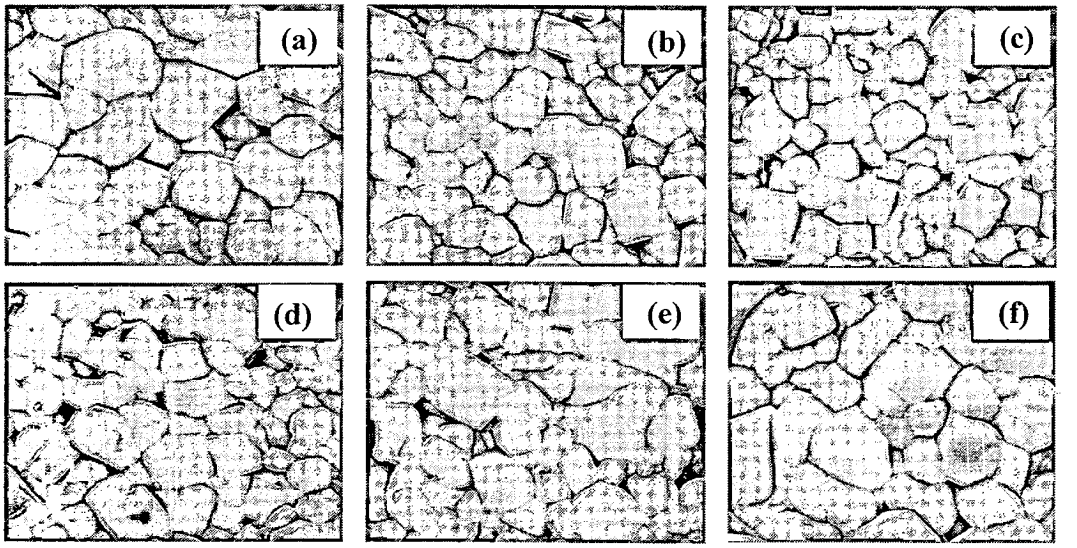

Figure 52 SEM images of BNKLT-x/y thermally etched surfaces with x= 0.18, (b) x=0.22, (c) x=0.26, (d)y=0, (e) y=0.07 and (f) y=0.10

Effect of x and y on electrical properties of BNKLT ceramics

I. Dielectric properties of BNKLT ceramics

Figure 53 and Figure 54 show the temperature dependence of the dielectric constant (ε_r) and dielectric loss (tanδ) of BNKLT-x/0.10 and BNKLT-0.20/y ceramics which were measured at different frequencies. All of the dielectric data feature, two dielectric anomalies, an obvious hump (at T_d) and a broad dielectric constant peak (at T_m) within the measuring temperature range were observed. The values for ε_r showeda pronounced dependence on frequency. With increased frequency, ε_r for all ceramics decreased. The tanδvalues reached a maximum value around T_d and no second dielectric loss peak occurs. The reason may be that tanδincreases sharply above T_m due to the high conductivity of the ceramics at high temperature [15]. Moreover, both T_d and T_m exhibit obvious dependence on the frequency. With increasing frequency, T_d moves to higher temperature regions and T_m moves to lower temperature regions. However, when the temperature is higher or lower than T_d and T_m, the ε_r does not show any evidence shift with increasing frequency. The broad ε_r peaks and the character of the temperature dependence of ε_r shows typical relaxation characteristics. A relaxor phase transition similar to what is seen in these compositions has been observed in many ABO_3-type perovskites and bismuth layer-structure compounds, such as (1-x)$Bi_{1/2}Na_{1/2}TiO_3$-x$BaTiO_3$[98], $Bi_{1/2}Na_{1/2}TiO_3$–$Bi_{1/2}K_{1/2}TiO_3$–$SrTiO_3$[99], $Bi_{1/2}Na_{1/2}TiO_3$–$Bi_{1/2}K_{1/2}TiO_3$ [1], of which either the A-sites or B-sites are occupied by at least two cations. For the BNKLT ceramics, Na^+, Bi^+, Li^+ and K^+ are randomly distributed in the 12-fold coordination sites, so the observed relaxor behavior is reasonably attributed to the disordering of the A-site cations and the compositional fluctuation.

Furthermore, T_d first decreased and then increased as the x and y content increased. This behavior may be attributed to the coexistence of a mixed rhombohedral-teragonal phase, which leads to more powerful stress in the MPB due to the incompatibility of their crystal lattices, resulting in a decrease of thermal stability in the long-range ferroelectric domains [100,101]. So, this is the reason of first decreases and then increases with increasing amount of x and y, which causes the lower depolarization temperature at the MPB compositions. In addition, the increase in deporarization temperature with the addition of BLT is important for

the application of BNT-based ceramics. The dielectric behavior of complex ferroelectrics with diffuse phase transition can be explained by the modified Curie–Weiss law according to the formula (13), where γ and C is assumed to be constant, γ value is between 1 and 2. When γ=1, the materials with this type phase transition can be called normal ferroelectrics; when 1 <γ< 2, the materials with this type phase transition are called relaxor ferroelectrics; whereas γ=2, the materials correspond to a so-called "complete" diffuse phase.

$$\frac{1}{\varepsilon} - \frac{1}{\varepsilon_m} = C(T - T_m)^{\gamma} \qquad (13)$$

Figure 55 shows the plot of $Ln(1/\varepsilon-1/\varepsilon_m)$ as a function of $Ln(T-T_m)$ for all ceramics samples at 1 kHz. The diffuseness exponent (γ) of ceramics is between 1.604 and 1.810 for composition of x (Figure 55(a)) and between 1.714 and 1.862 for compositions of y (Figure 55(b)), confirming that the BNKLT-x/y solid solutions exhibit diffuse phase transition behavior. These results imply an elevation of the relaxor nature with a transition from normal ferroelectric to relaxor ferroelectric behavior. This result was also observed in previous work prepared by the solid state method [15].

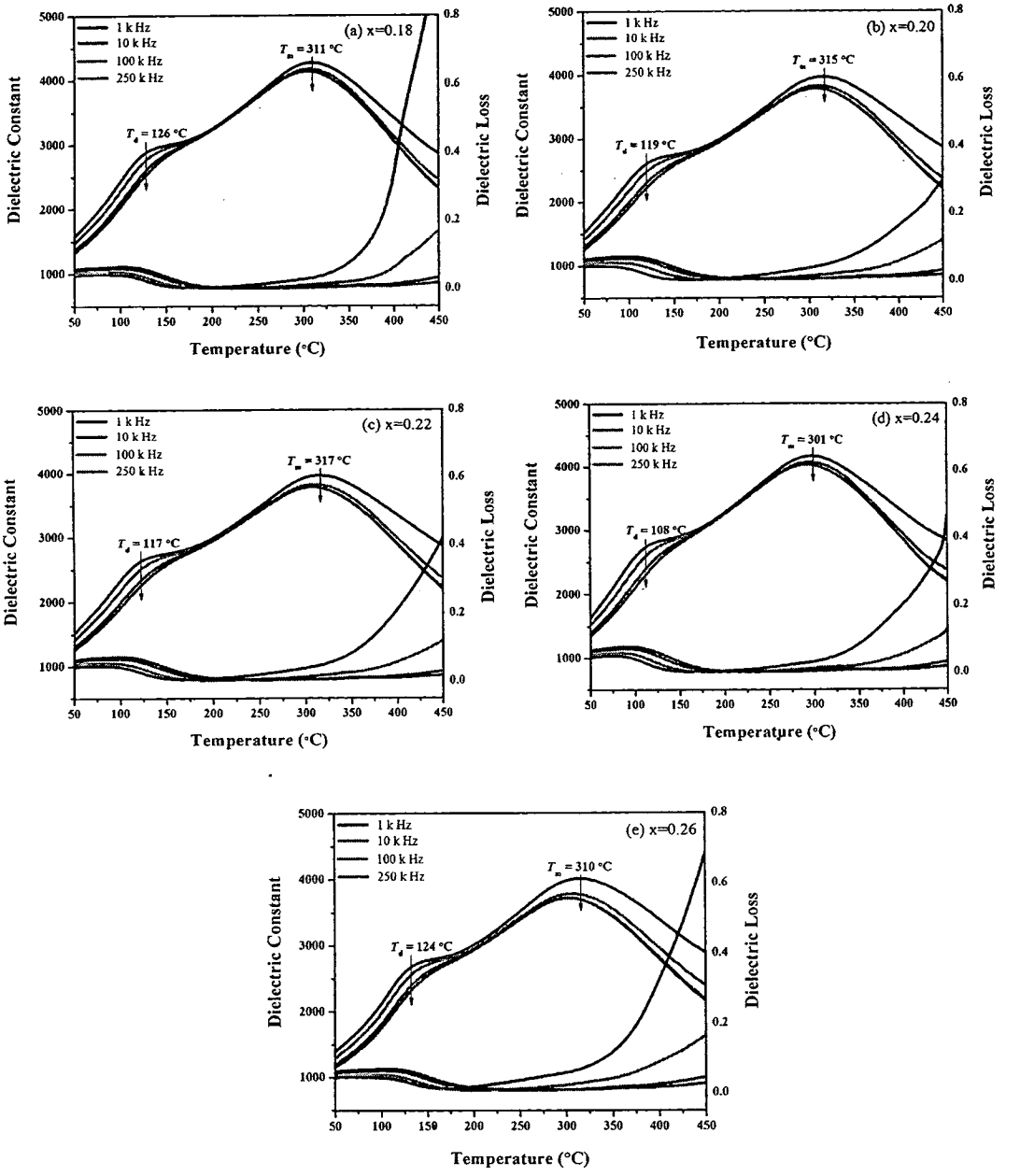

Figure 53 Temperature dependence of dielectric properties in the BNKLT system: (a) BNKLT-0.18/0.10, (b) BNKLT-0.20/0.10, (c) BNKLT-0.22/0.10, (d) BNKLT-0.24/0.10 and (e) BNKLT-0.26/0.10

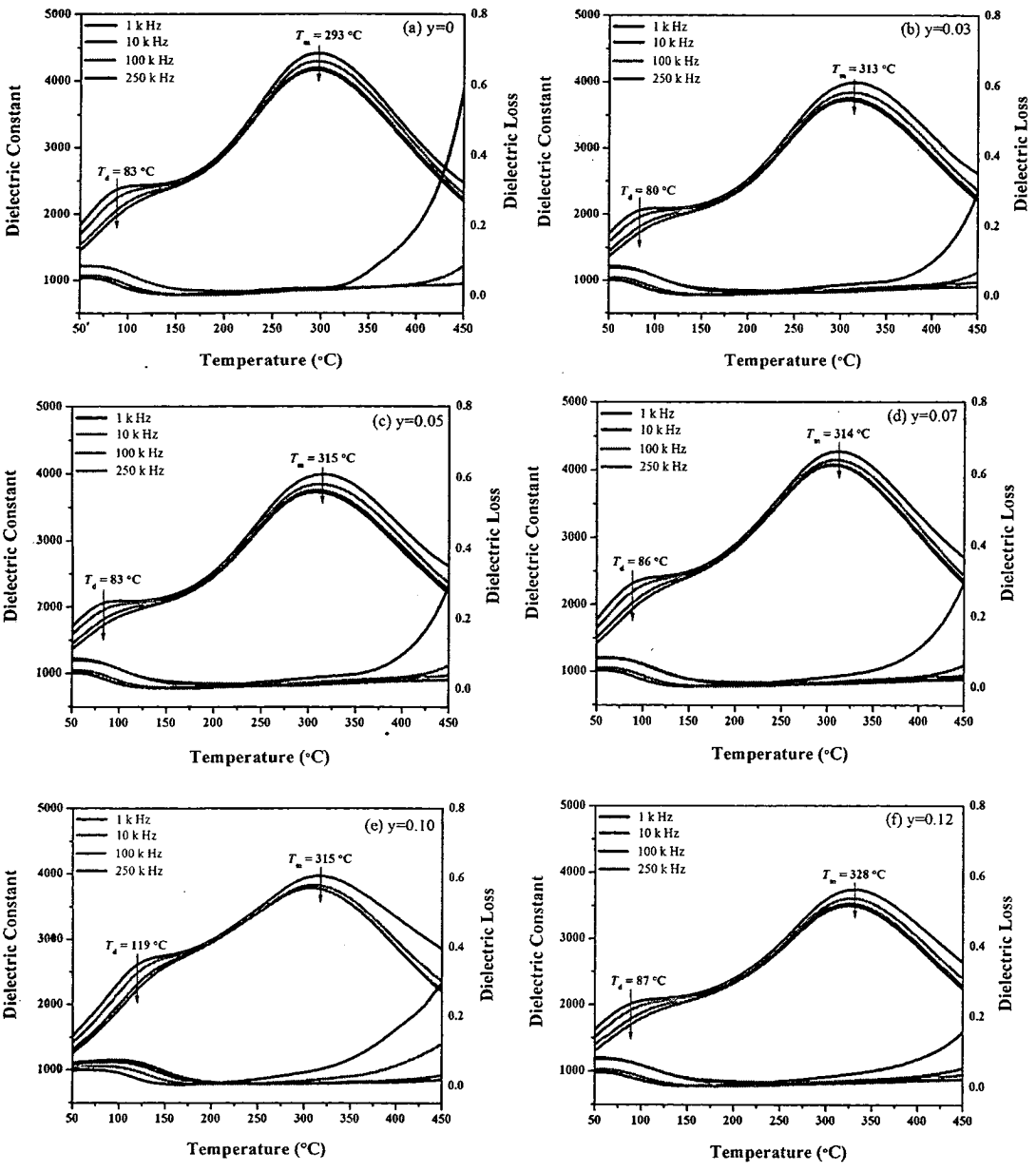

Figure 54 Temperature dependence of dielectric properties in the BNKLT system: (a) BNKLT-0.20/0, (b) BNKLT-0.20/0.03, (c) BNKLT-0.20/0.05, (d) BNKLT-0.20/0.07, (e) BNKLT-0.20/0.10 and (e) BNKLT-0.20/0.12

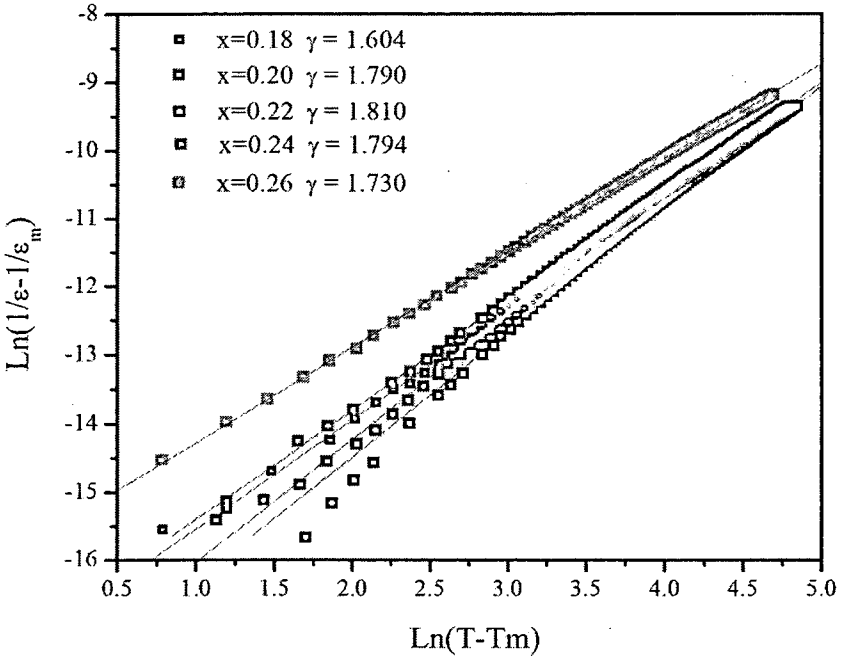

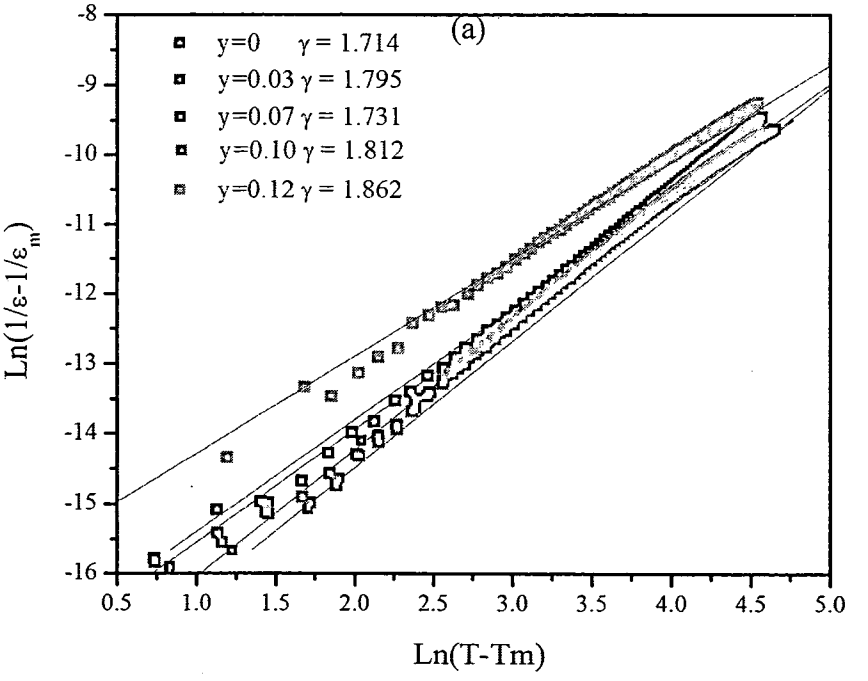

(b)

Figure 55 Logarithm of $(1/\varepsilon-1/\varepsilon_m)$ against logarithm of $(T-T_m)$ for the BNKLT system measured at 1 kHz (a) BNKLT-x/0.10 and (b) BNKLT-0.20/y

II. Ferroelectric properties of BNKLT ceramics

The P-E hysteresis loop of BNKLT-x/0.10 and BNKLT-0.20/y ceramics measured at 0.1 Hz is shown in Figure 56(a) and 7(b). At y=0, the polarization hysteresis loops display a well saturated typical ferroelectric behavior with the remnant polarization P_r and coercive field E_c of ~ 23.9 $\mu C/cm^2$ and ~21.0 kV/cm, respectively. However, with further increase in BLT (y=0.01, 0.03, 0.05, 0.07, 0.10 and 0.12), the coercive field (E_c) and the remnant polarization (P_r) both decrease rapidly and the P-E hysteresis loops become pinched and antiferroelectric-like behavior because of the coexistence of ferroelectric/non-ferroelectric phases and the transition between ferroelectric and relaxor phases under high electric field based on recent studies [101]). At y=0.10 and 0.12, the polarization hysteresis loop has become very weak and demonstrates paraelectric phase behavior. For compositions with BKT(x) content, hysteresis loops are not fully saturated in all composition. When there was increase of x content, hysteresis loops become more paraelectric (Figure 56(b) inset). The change of P-E loops indicates that the long-range ferroelectric order of the sample was disturbed and turned to the polar nano region (PNRs) with increased of x and y content. The value of P_r and E_c with x and y contents are shown in Table 15.

IV. Piezoelectric properties of BNKLT ceramics

The electromechanical strain (S-E) data for BNKLT-x/0.10 and BNKLT-0.20/y ceramics were measured at 0.1 Hz are presented in Figure 57(a) and Figure 57(b), respectively. At y=0, the S-E loops exhibit a butterfly shape, with negative strain of ~0.06% and a positive strain of ~0.22 % at 5 kV/mm which is typical for materials with ferroelectric order. With increase in y content, a decrease in negative strain could be observed with asignificant increase in usable positive strain up to 0.36 % at y=0.03, which is promising for the actuator application. For the sample with y>0.03, a gradual decrease in positive strain was observed. The same trend was found in the sample where x content was varied, as seen in Figure 57(b). From Figure 57(a) and 57(b), the variation of S_{max}/E_{max} of the ceramics with different y and x was shown (determined from the unipolar strain response under 0.1 Hz). For the compositions y=0, the S_{max}/E_{max} values are located at ~444 pm/V. When the BLT content is increased, the S_{max}/E_{max}values increase significantly and reaches ~727 pm/V for

the compositiony=0.03 due to the field-induced relaxor to ferroelectric phase transition.Aty>0.03, the value ofS_{max}/E_{max}decrease significantly. The results are in good agreement with the results of P-E hysteresis measurement. The same trend was found in the sample of x content, as seen in Figure 57(b). It is clear that the addition of y is highly effective at enhancing the performance with maximumS_{max}/E_{max} of ~729 pm/V for the y=0.03 composition in this system, which is comparable to leading lead free materials which have been reported [102-103].

The low-field piezoelectric coefficients (d_{33}) of BNKLT-x/0.10 and BNKLT-0.20/y ceramics are listedin Table 15. Thed_{33} values decreased slightly from 226 to129 pC/N with increasing of xcontent. Aty=0, the piezoelectric coefficients valuesd_{33} were 155 pC/N. With increasing content of y, d_{33} reached the maximum values of 219 pC/N at y=0.10, and then decreased in value. The d_{33} at y=0.10 showed a maximum value compared to the results of previous work prepared by the solid-state reaction method [15]. These results confirm that the combustion technique is a simple method for fabricating high quality BNKLT ceramics.

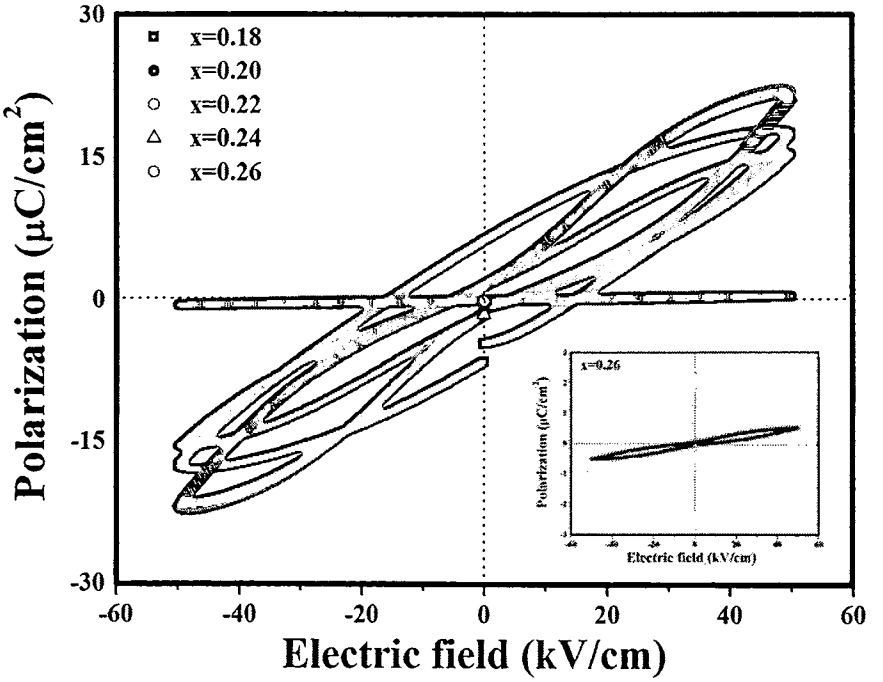

(a)

Figure 56 P-E hysteresis loop of (a) BNKLT-x/0.10 and (b) BNKLT-0.20/y ceramics measured at 0.1 Hz

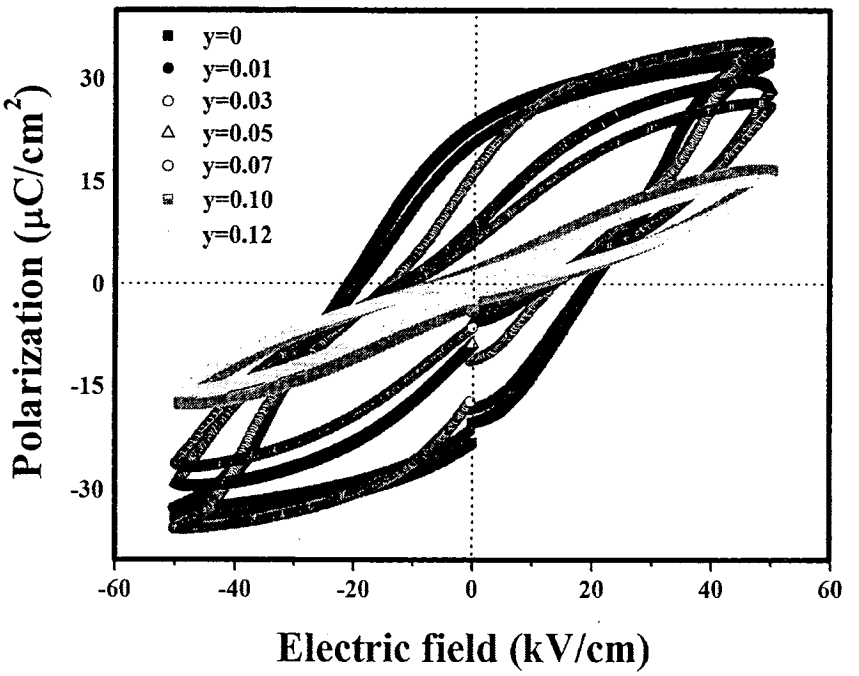

(b)

Figure 56 (cont.)

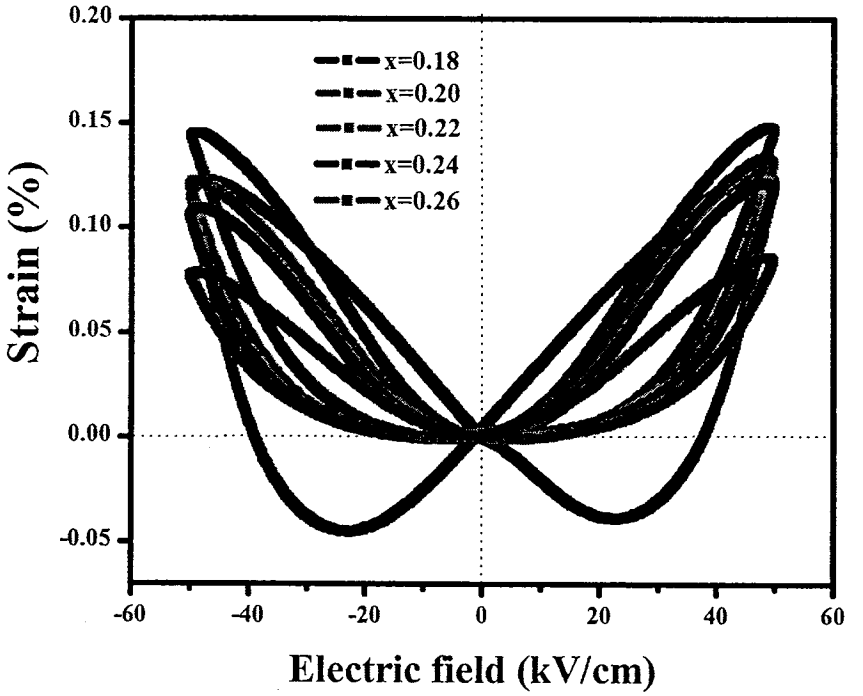

(a)

Figure 57 Strain loop of (a) BNKLT-x/0.10 and (b) BNKLT-0.20/y ceramics measured at 0.1 Hz

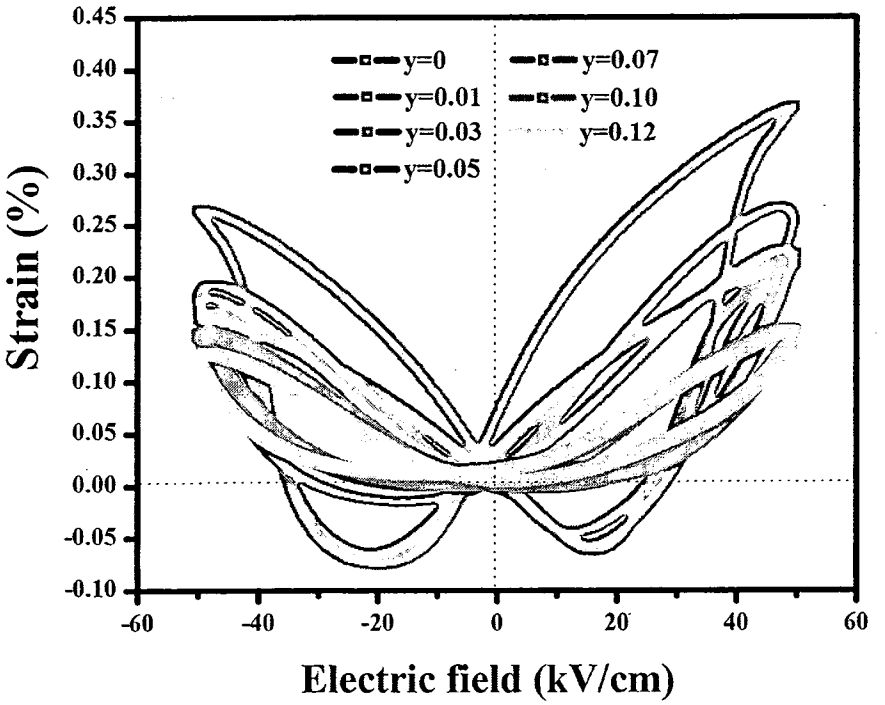

(b)

Figure 57 (cont.)

Table 15 Average grain size, T_d, T_m, P_r, E_c, S_{Max}, S_{Neg}, S_{Max}/E_{Max} and d_{33} of BNKLT-x/y ceramics

Composition	Average grain size (μm)	T_d (°C)	T_m (°C)	γ	P_r (μC/cm^2)	E_c (kV/cm)	Strain (%)		S_{Max}/E_{Max} (pm/V)	d_{33} (pC/N)
							S_{Max}	S_{Neg}		
x=0.18	1.34	126	311	1.604	6.37	14.9	0.12	0.03	239	226
x=0.20	1.23	119	315	1.790	1.51	6.3	0.14	0.003	294	219
x=0.22	1.33	117	317	1.810	1.47	4.5	0.13	0.002	270	167
x=0.24	1.04	108	301	1.794	1.47	4.4	0.12	0.001	234	132
x=0.26	0.81	124	310	1.730	-	-	0.08	0.001	169	129
y=0	0.97	83	293	1.714	23.9	21.0	0.22	0.066	444	155
y=0.03	1.05	80	313	1.795	16.6	18.8	0.36	0.045	727	159
y=0.05	1.17	83	315	1.795	9.09	13.8	0.26	0.003	559	175
y=0.07	1.20	86	314	1.731	6.80	12.1	0.22	0.003	486	180
y=0.10	1.33	119	315	1.812	2.71	11.9	0.14	0.003	294	219
y=0.12	1.81	87	328	1.862	1.59	5.19	0.14	0.001	283	111

Conclusions

BNKLT ceramics were prepared by the combustion technique with optimum calcination and sintering of 750 and 1025 for 2 h. The firing temperatures have direct effect on phase formation, grain size, densification microstructure and dielectric properties of ceramic samples. The structure exhibited the coexistence of rhombohedral and tetragonal phases, which is consistent with the nature of the specimen with an MPB composition. The optimum sintering temperature significantly promoted the grain growth and microstructure densification. The highest dielectric at T_c (ε_r = 4,344) and density (ρ = 5.79 g/cm^{-3}) were obtained from the sample sintered at 1025 °C. These results were higher than the sample obtained by solid state reaction method and confirmed that the combustion technique has potential to fabrication of high purity BNKLT ceramics using lower firing temperature.

The addition of BKT (x) and BLT (y) directly affect the crystal structure, microstructure, density and electrical properties. The crystal structure shows the coexistence of rhombohedral and tetragonal phases at the MPB composition BNKLT-0.20/0.03. The SEM result indicated with increasing x content, the grain size decrease. But with increasing y content, the variation of the grain size is opposite. The dielectric spectra show two distinct phase transitions approximately 110 °C and 310 °C. All the samples show relaxor behavior which is linked to the presence of disorder on the A-site. The coexistence of a polar and non-polar phase at the MPB was indicated by a pinched P-E loop and a large strain of ~0.36% at the composition BNKLT-0.20/0.03 with S_{max}/E_{max}~729 pm/V. These large strains in combustion-prepared samples represent a significant improvement on solid-state prepared samples and shows great promise for actuator application.